
In-situ interferometric monitoring of digital light processing based two-material Vat photopolymerization

Yue Zhang, Haolin Zhang, Xiayun Zhao*

Department of Mechanical Engineering and Materials Science, University of Pittsburgh

* Email: xiayun.zhao@pitt.edu

Abstract

Vat photopolymerization process (VPP) is increasingly used for multi-material 3D printing via either conventional multi-vat switchover mechanism or emerging multi-wavelength selective curing. In-situ monitoring techniques are much desired to advance the precision in VPP and enhance its applicability to fabricating sophisticated components such as flexible electronics and soft robots. This work is aimed to develop a non-destructive in-situ interferometric curing monitoring (ICM) framework to monitor a distinct digital light processing process that employs wavelength-selective photopolymerization mechanism. Machine learning aided data analytics method is developed to process the ICM-acquired interferogram data, alongside a physics sensor model to estimate each voxel's average refractive index. Then, a model is developed by correlating the refractive index to the degree of curing (DoC) for revealing the spatial variation of material properties in a study case of two-material VPP. Our experiment results show that the developed ICM method can provide real-time insights about the multi-material VPP process dynamics and output, paving a way for closed-loop feedback control to improve the process reproducibility.

Keywords: Vat photopolymerization, non-destructive in-situ monitoring, Interferometry

1. Introduction

Additive Manufacturing (AM) technologies could create objects with less material waste and higher efficiency compared to traditional manufacturing methods. One commonly used AM method is Digital light processing (DLP) based vat photopolymerization process (VPP). In this process, a 3D model created by computer software is sliced into cross-section images that are used to generate optical masks by a digital micromirrors device (DMD) and projected into a resin chamber. The masks are projected into a resin chamber one by one, solidifying layer by layer until a 3D object is created. VPP enables the printing of objects with different mechanical properties. Schwartz et al. developed a multicomponent resin that utilizes a dual-wavelength DLP printer to selectively produce stiff and soft parts by controlling the each wavelength light beam's exposure setting [1]. The resin consists of acrylate and epoxide-based monomers along with their corresponding initiators. While visible light only induces the curing of the acrylate monomer to create soft objects, UV light can cure both the acrylate and epoxide monomers, resulting in objects with higher Young's modulus. However, a lack of an in-situ monitoring method for multi-wavelength printing hinders a comprehensive understanding of the curing process during the multi-wavelength DLP based VPP. To gain a better understanding and enhance control over the process dynamics and in-process part properties in VPP printing, it is necessary to develop an in-situ monitoring system to visualize the curing process dynamics and estimate the printed part's properties, such as refractive index and degree of conversion. Degree of conversion (DoC) is an important internal variable in the photopolymerization process as it increases with the crosslinking of monomers and critically determines the mechanical properties of printed parts. To monitor the evolution of DoC in the curing process, we have been developing an in-situ interferometric curing monitoring

(ICM) system. Existing monitoring methods for VPP include atomic force microscopy (AFM), Fourier-transform Infrared Spectroscopy (FT-IR) and Schlieren imaging, which, however, come with certain limitations [2-5]. AFM and FT-IR methods are destructive and expensive to implement, while Schlieren imaging requires complex optics and has a limited view that cannot cover the full curing area. Our ICM system is non-destructive, low-cost and can be easily integrated with the DLP printer. The basic idea for DLP-VPP process monitoring using ICM originates from the research conducted by Zhao et al [6-10]. In their works, they developed an interferometric curing monitoring and measurement (ICM&M) method that employed the multi-beam interference model and adaptive estimation of instantaneous frequency to quantify the cure height of in-process samples. Their method was successfully implemented in an exposure-controlled projection lithography (ECPL) process [6-10]. Herein, the objective of our project is to adapt and extend the ICM&M method for in-situ monitoring of the refractive index and DoC during a wavelength selective polymerization based two-material VPP process. To estimate the refractive index from the interferogram video, we developed an explicit model based on the multi-beam interference optics utilized in the DLP-VPP system. Additionally, a machine learning-based outlier detection model is employed to identify pixels that are less affected by noise, which may be induced from the movement and shrinkage of the liquid resin during the DLP-VPP process. To predict the DoC, a linear correlation model between refractive index and DoC will be developed to predict DoC during the curing process.

2. Methodology

2.1. Two-wavelength DLP-VPP process

As Figure 1 shows, our two-wavelength DLP-VPP printer includes two commercial DLP projectors (PRO4500, Wintech Digital, Carlsbad, CA) with different light sources. One is equipped with an ultraviolet (UV) light LED whose wavelength

is 365 nm and another is equipped with visible light source with a wavelength of 460 nm.

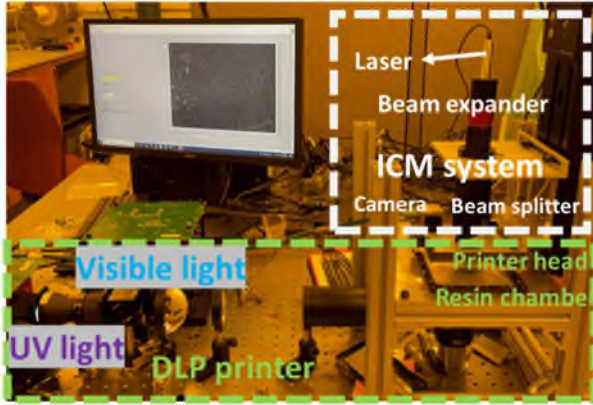


Figure 1. Our two-wavelength DLP-VPP system for multimaterial printing and in-situ ICM system for the process monitoring

2.2. Materials

The multicomponent resin used in this project is adapted from Schwartz's material system [1]. The resin is prepared using the acrylate-based monomer 2-hydroxyethyl acrylate (HEA), epoxide-based monomer 3,4-epoxycyclohexylmethyl-3,4-epoxycyclohexane carboxylate (EPOX), the free radical initiator Irgacure 819 ($\lambda_{cutoff} = 450$ nm) and cationic initiator triarylsulfonium salts (TAS, $\lambda_{cutoff} = 390$ nm). All the chemicals were purchased from Sigma-Aldrich. All the materials were used as received without any additional modifications.

2.3. Experiment design

The specimens were designed as a circle shape with a diameter of 2.5 mm. In the printing process, only a single layer is printed, and the initial position of the print head is set as 133.8 mm, the print head is moved with a linear travel motorized stage (LTS-150, Thorlabs, Newton, NJ). The UV light exposure time is 20 seconds and visible light exposure time is 60 seconds. The light intensities used to print specimens is 11.82 mw/cm^2 and 15.48 mw/cm^2 . The power of the light mask is measured via an optical power meter (PM400, Thorlabs, NJ, USA) directly on the projection window (Quartz glass slide, Alpha Nanotech Inc, BC,

Canada). The area of light masks on projection window is measured by a digital calliper with a resolution of 0.01 mm. then the light intensity is calculated by the $\frac{\text{light power}}{\text{light mask area}}$.

2.4. In-situ interferometric monitoring of two-material VPP

The ICM system is shown in Figure 1, which including a CMOS camera (acA2040-120um, Basler, Exton, PA) with a sampling frequency of 120 Hz, a collimated green laser of wavelength of 532 nm (CPS532, Thorlabs, Newton, New Jersey), a beam expander (GBE10-A, Thorlabs, Newton, New Jersey) and a 50:50 (R:T) split ratio beam splitter (BS013, Thorlabs, Newton, New Jersey). The optics and camera is fixed above the moving print stage by a 3D printed fixture.

Figure 2 show the overview of the DLP-specific ICM system, The workflow is as follows. 1) Design an ICM system. 2) Develop an explicit model for refractive index estimation from recorded interferogram video. 3) Pre-processing time series of grayscale value with filters. 4) Develop a machine learning model to detect good pixels and use the good pixels to estimate the average refractive index. 5) Calibrate the correlation model between ICM-derived refractive index and DoC. 6) Validate the developed ICM method to estimate refractive index and predict DoC.

For data preprocessing, a 5×5 image median filter is applied to the raw frames to reduce noise. Additionally, for each time series of grayscale values, a low-pass filter with a cut-off frequency of 5 Hz is employed to eliminate high-frequency noise. This is followed by applying a MATLAB moving average filter to smoothen the curve for enhancing the accuracy of curve fitting results. The cut-off frequency of the low-pass filter is determined based on the signal frequency.

To identify reliable pixels for further data processing, a robust and accurate outlier detection method is developed via machine learning (ML). In the interferogram video, certain pixels may be affected by noise caused by the movement of the print stage and resin flow during polymerization, making them unreliable for providing accurate information. To distinguish between good pixels and noisy pixels (referred to as outliers in this work), an ML-assisted algorithm is developed and applied for pixel classification. The algorithm utilizes a specific pattern to identify and utilize good pixels for subsequent data processing, while marking bad pixels as outliers. A one-dimensional neural network is trained and tested for this purpose.

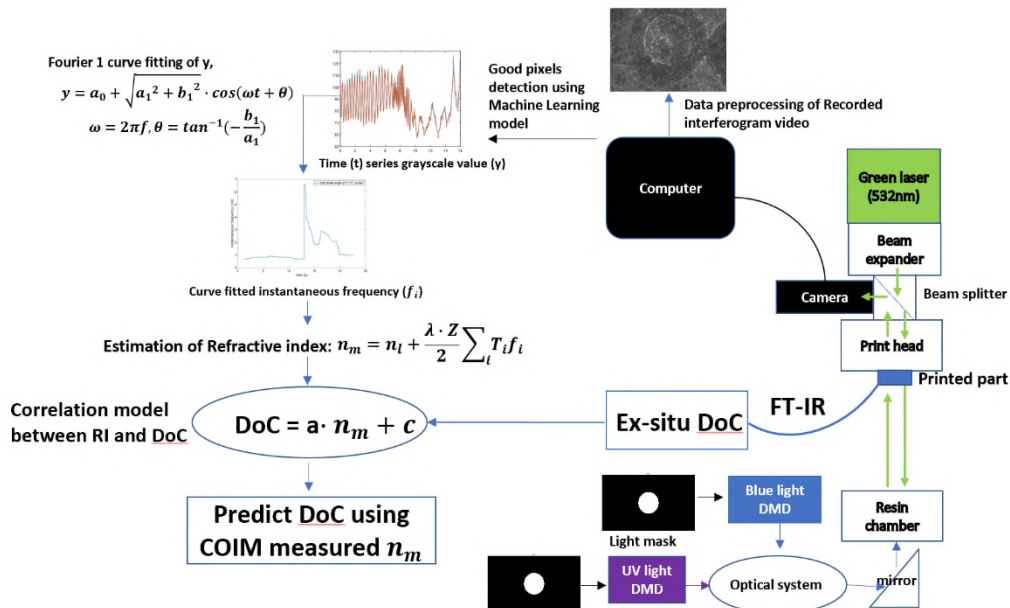


Figure 2. The developed framework of their-situ interferometric monitoring for digital light processing based vat photopolymerization processes

An explicit sensor model for the DLP-ICM system is developed based on multi-beam interference optics shown in Figure 3. The assumption is made that for each layer, the cured layer has grown refractive index and the fixed cured height (i.e., layer thickness).

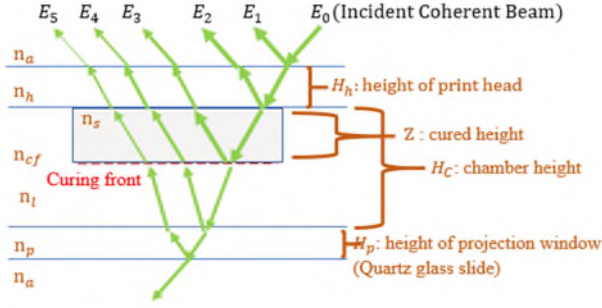


Figure 3. The multi-beam interference optics model for a DLP-VPP specific ICM that shines a measurement light beam from beneath the print stage (Note: in this work, we irradiate the measurement light beam from the top instead. Hence, the model shown here should be inverted for our actual ICM setup in Fig. 1). $n_a, n_p, n_i, n_{cf}, n_s, n_h$ are refractive index of air, projection window, liquid resin, curing front, cured solid part, print head, respectively. The schematic was adapted from [8]

According to Figure 3, the total wave in equation 2 can be obtained by summing vectors of the light wave components in Equation 1, where A_n is the real positive amplitude, and ϕ_n is the phase angle of each wave [4].

$$E_n = A_n e^{i\phi_n}, n = 1, 2, \dots, 5 \quad 1$$

$$E_T = \sum_{n=1}^5 E_n = \sum_{n=1}^5 A_n e^{i\phi_n} \quad 2$$

When the field is observed using a CMOS camera, the resulting measurement is the average of the field energy per unit area over the integration time of the camera. This measurement is referred to as irradiance I [11], which is proportional to the squared module of the amplitude, as shown in equation 3 [4].

$$I = |E_T|^2 = \left| \sum_{n=1}^5 A_n e^{i\phi_n} \right|^2 \quad 3$$

$$= \sum_{n=1}^5 |A_n|^2 + 2 \sum_{j=1}^5 \sum_{k=1, k \neq j}^5 A_j A_k \cos(\delta_{jk})$$

Where $\delta_{jk} = \phi_j - \phi_k$, is the relative phase difference between the component of each wave, caused by optical path length differences between each set of two wave components [4].

The camera observed intensity I_M is shown in sensor model, equation 4 and 5 [4], where f is caused by curing process, $f = \frac{2(n_m - n_i) dZ}{\lambda dt'}$

$$I_M = I_0 + I_1 \cos(\delta + \varphi)$$

$$\omega = 2\pi f = \frac{d(\delta + \varphi)}{dt} = \frac{d\delta}{dt} = \frac{4\pi(n_m - n_i) dZ}{\lambda dt}$$

A differential form of the cured height is derived from equation 5 to get the equation 6 [4].

$$\frac{dZ}{dt} = \frac{\lambda}{2(n_m - n_i)} \left(f - \frac{2\pi n_i dH_C}{\lambda dt} \right) \quad 6$$

Then the explicit ICM sensor model is generated using Euler's Method shown in equation 7 [4],

$$n_m = n_l + \frac{\lambda \cdot Z}{2} \sum_i T_i f_i \quad 7$$

To solve the sensor model shown in Equation 7. The estimation of instantaneous frequency f is necessary, which is achieved using a parameter estimation algorithm that applies an exponentially weighted moving horizon window Fourier curve fitting. The algorithm works by fitting a Fourier curve to the data within a moving window. The weights assigned to the data points exponentially decrease as they move further away from the current point, so recent data points have a stronger influence on the curve fitting process compared to older data points. The window size in the fitting process is adaptively adjusted based on the data. Initially, a window size of 120 frames is used. However, if the R-squared value (a measure of the goodness of fit) falls below 0.9, indicating a poor fit, the window size is modified. The algorithm continues to adjust the window size until a better fitting result is achieved. The principle of this algorithm is to extract the instantaneous frequency using "Fourier 1" Curve fitting as equation 8 and integrates the instantaneous frequency in the curing process to get the total phase angle. Then using the developed sensor model, equation 7 to calculate refractive index of voxel in the region of interest.

$$y = a_0 + a_1 \cdot \cos(\omega t) + b_1 \cdot \sin(\omega t)$$

$$= a_0 + \sqrt{a_1^2 + b_1^2} \cdot \cos(\omega t + \theta) \quad 8$$

Where t is time, $\omega = 2\pi f$, $\theta = \tan^{-1}\left(-\frac{b_1}{a_1}\right)$

3. Results and discussion

As a preliminary study, two samples are cured using different wavelengths: UV light and visible light. The exposure time for UV light cured sample is 20 seconds and the exposure time for visible light cured sample is 50 seconds. FT-IR is employed to measure the DoC of the cured samples to establish a linear model between refractive index and DoC. However, the obtained FT-IR spectra did not provide satisfactory results due to weak absorption at the absorption mode. In future experiments, the transmission mode in FT-IR and photo-differential scanning calorimetry (DSC) will be tested as alternative methods to measure the DoC. Figure 4 displays the sample pictures and corresponding interferogram video pictures, illustrating the difference between the visible light-cured sample and the UV light-cured sample. The UV light-cured sample appears larger and requires a shorter exposure time. This can be attributed to the higher absorption of the radical initiator, Irgacure 819, at the UV light wavelength. The measured dimensions of two samples and corresponding pixel numbers in the interferogram video were shown in Table 1, the pixel numbers were calculated from the length of orange line shown in Figure 4.

Table 1. Sample dimensions

Sample description	Thickness (mm)	Diameter (mm)	Number of pixels in ICM video
UV cured sample	0.34	2.64	171
Visible light cured sample	0.46	1.66	85

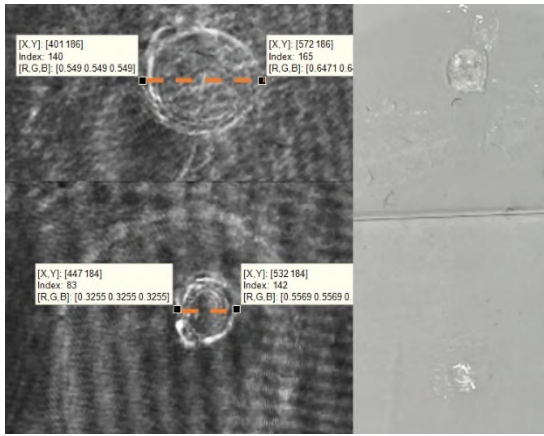


Figure 4. One frame of ICM interferogram video and sample photos. Top: UV light cured sample, bottom: visible light cured sample.

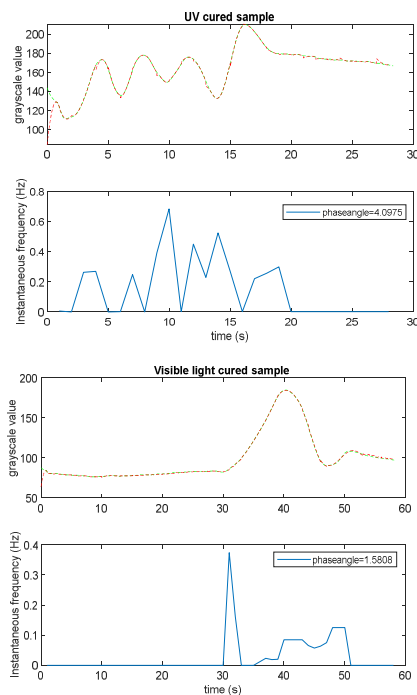


Figure 5. Time series grayscale value of representative voxel in Top, UV light cured sample, bottom, visible light cured sample and their estimated instantaneous frequency.

Based on the information extracted from the obtained interferogram video, there are observable differences in the curing process between different wavelengths. Figure 4 and Figure 5 display representative pixels selected from interferogram videos of the UV cured sample and visible light cured sample, respectively. For UV-cured sample, the incubation time is shorter, approximately 2 seconds, compared to the visible light-cured sample, which has an incubation time of up to 30 seconds. Additionally, the visible light-cured sample exhibits a lower phase angle of 1.5808 compared to the UV light-cured sample's value, 4.0975. This discrepancy can be attributed to the difference in optical path length through the two samples. Note that the blue light cured sample exhibits a smaller phase angle compared to the UV sample but a greater cured thickness (Table 1). This is suspected to be due to a lower DoC and a lower refractive index in the visible light-cured sample. More conclusive work will be reported after a further study.

4. Conclusion

The goal of the project is to develop an in-situ interferometry system for a dual-wavelength DLP based VPP to achieve an in-situ monitoring of refractive index and prediction of DoC in a multi-material printing process. The ICM system could be further improved to provide real-time, close-loop feedback control of the two-material vat photopolymerization process, thus improving the fidelity and reproducibility of the parts being cured. In the future, a machine learning-based model will be enhanced for the outlier detection process. The refractive index of the liquid resin will be calibrated to evaluate the refractive index of cured parts. Further, the transmission mode of FT-IR and photo DSC will be used to characterize DoC of printed parts. Then a correlation model between DoC and refractive index will be developed for achieving the ultimate goal of predicting DoC during wavelength selective multi-material VPP.

Acknowledgments

This work has been supported by the National Science Foundation under Faculty Early Career Development Award: CMMI-2238557.

References

- [1] J. J. Schwartz and A. J. Boydston, "Multimaterial actinic spatial control 3D and 4D printing," *Nat Commun*, vol. 10, p. 791, Feb 15 2019.
- [2] C. I. Higgins, T. E. Brown, and J. P. Killgore, "Digital light processing in a hybrid atomic force microscope: In Situ, nanoscale characterization of the printing process," *Additive Manufacturing*, vol. 38, 2021.
- [3] T. Hafkamp, G. van Baars, B. de Jager, and P. Etman, "A feasibility study on process monitoring and control in vat photopolymerization of ceramics," *Mechatronics*, vol. 56, pp. 220-241, 2018.
- [4] A. Chivate and C. Zhou, "Enhanced Schlieren System for In Situ Observation of Dynamic Light-Resin Interactions in Projection-Based Stereolithography Process," *Journal of Manufacturing Science and Engineering*, vol. 145, 2023.
- [5] C. Chung Li, J. Toombs, and H. Taylor, "Tomographic color Schlieren refractive index mapping for computed axial lithography," presented at the Symposium on Computational Fabrication, 2020.
- [6] R. E. Schwerzel, A. S. Jariwala, and D. W. Rosen, "A simple, inexpensive, real-time interferometric cure monitoring system for optically cured polymers," *Journal of Applied Polymer Science*, vol. 129, pp. 2653-2662, 2013.
- [7] X. Zhao and D. W. Rosen, "Experimental validation and characterization of a real-time metrology system for photopolymerization-based stereolithographic additive manufacturing process," *The International Journal of Advanced Manufacturing Technology*, vol. 91, pp. 1255-1273, 2016.
- [8] X. Zhao and D. W. Rosen, "Real-time interferometric monitoring and measuring of photopolymerization based stereolithographic additive manufacturing process: sensor model and algorithm," *Measurement Science and Technology*, vol. 28, 2017.
- [9] X. Zhao and D. W. Rosen, "A data mining approach in real-time measurement for polymer additive manufacturing process with exposure controlled projection lithography," *Journal of Manufacturing Systems*, vol. 43, pp. 271-286, 2017.
- [10] X. Zhao and D. W. Rosen, "An implementation of real-time feedback control of cured part height in Exposure Controlled Projection Lithography with in-situ interferometric measurement feedback," *Additive Manufacturing*, vol. 23, pp. 253-263, 2018.
- [11] C. Meneses-Fabian and U. Rivera-Ortega, "Phase-shifting interferometry by wave amplitude modulation," *Optics Letters*, vol. 36, pp. 2417-2419, 2011/07/01 2011.